BOLETIN DE LA SOCIEDAD ESPAÑOLA DE
Cerámica y Vidrio
www.elsevier.es/bsecv

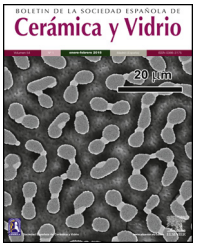

Original

Nanostructured MgO-enhanced catalytic ozonation of petrochemical wastewater

Leili Mohamadi[a], *Edris Bazrafshan*[b], *Abbas Rahdar*[c], *Geórgia Labuto*[d], *Ali Reza Kamali*[e,*]

[a] *Infectious Diseases and Tropical Medicine Research Center, Zahedan University of Medical Sciences, Zahedan, Iran*
[b] *Faculty of Health, Torbat Heydariyeh University of Medical Sciences, Torbat Heydariyeh, Razavi Khorasan, Iran*
[c] *Department of physics, university of Zabol, Zabol, Iran*
[d] *Chemyistry Department, Universidade Federal de São Paulo, São Paulo, Brazil*
[e] *Energy and Environmental Materials Research Centre (E²MC), School of Metallurgy, Northeastern University, Shenyang 110819, People's Republic of China*

ARTICLE INFO

Article history:
Received 26 February 2020
Accepted 8 June 2020
Available online 29 June 2020

Keywords:
Petrochemical contaminants
Catalytic ozonation
MgO
Nanoparticles

ABSTRACT

Petrochemical wastewater, which is a complex solution of various chemicals, can cause severe environmental problems after being disposed to environment. Here, we investigate the removal of petrochemical contaminants at different periods and pH levels using three distinct processes: conventional ozonation, adsorption and nanostructured MgO-enhanced catalytic ozonation. The latter is found to be an economical and efficient new approach to treat petroleum contaminants, outperforming the other methods. For instance, after 30 min of the treatment using the conventional ozonation, the removal percentages of benzene, toluene, ethylbenzene, and xylene are 35, 58, 81, and 92%, respectively; whereas the corresponding figures are 93.8, 83.5, 94.6, and 99.2% using the catalytic ozonation.

Tratamiento catalítico de ozono de aguas residuales petroquímicas impulsado por nanoestructuras MgO

Palabras clave:
Contaminantes petroquímicos
Zona catalítica
MgO
Nanopartículas

RESUMEN

Las aguas residuales petroquímicas, que es una solución compleja de diversos productos químicos, pueden causar graves problemas ambientales después de ser eliminadas en el medio ambiente. Aquí, investigamos la eliminación de contaminantes petroquímicos en diferentes periodos y niveles de pH utilizando tres procesos diferentes: zona convencional, adsorción y ozono catalítico mejorado por nanoestructuras MgO. Este último es visto como un nuevo enfoque económico y eficiente para el tratamiento de los contaminantes del petróleo, superando a otros métodos. Por ejemplo, después de 30 minutos de tratamiento

* *Corresponding author.*
E-mail address: ali@smm.neu.edu.cn (A.R. Kamali).
https://doi.org/10.1016/j.bsecv.2020.06.002

utilizando ozono convencional, las tasas de eliminación de benceno, tolueno, etilbenceno y xileno son 35, 58, 81 y 92%, respectivamente; mientras que las cifras correspondientes son 93, 8, 83,5, 94,6 y 99,2% utilizando ozonación catalítica.

Introduction

Hazardous chemicals such as benzene, toluene, ethylbenzene, and xylene, which naturally exist in crude oil and gasoline, can easily be transferred into surface and groundwater due to either the leakage from industrial petrochemical equipment or inappropriate waste disposal [1,2]. Considering that the petroleum industry consumes large volumes of water, especially for cooling purposes, a large amount of petrochemical wastewater is produced [3,4]. Therefore, the appropriate treatment of polluted water sources produced in such industries is a challenge. Not to mention that the disposal of untreated petrochemical wastewater can cause grave environmental issues [5], expanding the presence of contaminants such as phenols and toxic hydrocarbons in the environment [6].

In general, wastewater from petroleum refineries contains large quantities of environmentally problematic materials; somewhere around 150-250 mg/L BOD (Biological Oxygen Demand), 150-250 mg/L COD (Chemical Oxygen Demand) and 20-200 mg/L phenols, as well as 100-300 mg/L other petroleum products and 5000 mg/L salts [7], disrupting habitats of human and also wildlife communities [8,9]. The disposal of such wastewaters might destroy a considerable number of the biotic elements, leading to the gradual elimination of aquatic plants and animal species. It also simplifies the food chain through reducing the number and diversity of species [10]. Therefore, organic and inorganic contaminants present in petrochemical wastewaters must be carefully treated and removed, before the wastewater can be discharged into the environment [11]. A variety of methods have been suggested, and used, for the removal of petroleum contaminants from water resources, including chemical coagulation and sedimentation, filtering, photocatalytic oxidation, and adsorption [12]. Unfortunately, the appropriate implementation of such technologies is often very expensive, complicated and time-consuming, providing various challenges particularly in developing countries [13].

Advanced oxidation processes (AOPs) are among the most effective methods for the removal of organic contaminants. These methods are based on the production of highly oxidizing free radicals such as hydroxyl radicals, capable of mineralizing various toxic organic compounds [14]. AOPs are operationally easy, low cost, and efficient while being able to stabilize organic compounds through converting them into water and carbon dioxide [15–18] often using ozone [19]. APOs are suitable for treating contaminants that are resistant to biological decomposition [20,21].

Catalytic ozonation processes (COPs) are APOs in which solid catalysts play a role in overall ozonation process, facilitating the decomposition of ozone into free radicals. In fact, the use of catalysts may eliminate the most important limitations of simple ozonation, including the low solubility and stability of ozone in water, and its slow reaction with organic compounds [22,23]. The high efficiency, as well as low operation costs influenced by the short duration of COPs [24,25] also facilitates the implementation of these technologies, particularly, in developing countries.

Metal oxides, such as magnesium oxide (MgO) nanoparticles, have a high potential to be used in wastewater treatments, due to their possible large surface areas and the low cost of recovery and production. MgO also provides advantages of having antibacterial properties and high adsorption and/or photocatalysis performance for toxic compounds [26–28].

Various studies have been conducted on using MgO in COPs for the removal of toluene [29], textile dyes [30] and humic acid [31]. Moosavi et al. [32] studied the effect of MgO-enhanced COP on the removal of Reactive Red198, indicating that the removal efficiency improves with the increase of the pH value, due to the increased rate of ozone decomposition into free radicals at higher pH values. The decomposition of the dye molecules was attributed to an indirect oxidation process brought about by the active radicals. The present research intends to study the feasibility of using MgO nanoparticles in COP for the effective treating of petrochemical wastewater.

Materials and methods

Real wastewater samples were provided by a large petrochemical unit located in southern Iran. All other chemicals used in the research were of high purity and manufactured by the German Company Merck. The wastewater experiments were conducted using a laboratory scale semi-continuous ozonation reactor, shown in Fig. 1.

Before performing water treatment processes, the wastewater sample was tested to determine the values of COD, BOD, TS (Total Solid), and turbidity, as well as the amounts of benzene, toluene, ethylbenzene, and xylene. For this, 1 μL of the wastewater was injected into an Agilent's Gas Chromatography (GC) with the GC column HP-5 30m, and 0.50 μm film thickness using a flame-ionization detector. The incubator temperature was maintained at 40 °C for 10 min before the injection. The extraction was performed at 120°C and 500 rpm. The initial furnace temperature was kept at 40°C for 2 min, gradually raised to 80°C at the rate of 20°C/min, and kept at this temperature for 1 min. The temperatures of the injector and detector were set at 250 and 300°C, respectively, and nitrogen gas flow rate was maintained constant at 3 mL/min. The amount of each component was calculated through comparing the diagram provided by the GC machine with that obtained by injecting standard samples into the GC

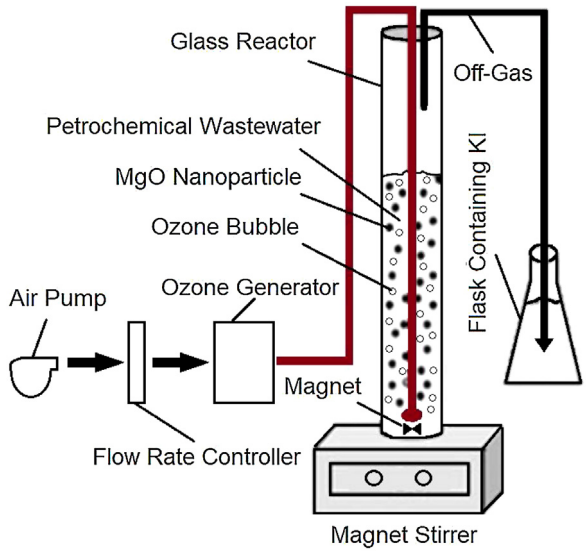

Fig. 1 – Schematic representation of the reactor used for the petrochemical wasterwater treatment in the presence of MgO nanoparticles.

Table 1 – Characteristics of the petrochemical wastewater collected from an Iranian petrochemical industry.

Value	Parameter
7.5	pH
1355 mg/l	COD
395 mg/l	BOD5
3.43	COD/BOD5
2464 mg/l	TS
780 NTU	Turbidity

equipment. Table 1 represents the characteristics of the petrochemical wastewater used in this study.

Preparation of MgO nanocatalysts

MgO nanoparticles, used as nanocatalysts in the wastewater treatment, were prepared by the calcination approach. For this, Mg $(NO_3)_26H_2O$ was first dried at 100 °C for 8 h. Then, the dried powder was calcined at 500°C for 2 h in an electrical furnace to form MgO nanoparticles. The morphology of nanoparticles was studied using scanning (SEM), and transmission (TEM) electron Microscopy. A Philips X-ray diffractometer (XRD) with Cu-Kα radiation (1.54 Å) was employed for the structural study.

Catalytic ozonation process (COP)

A semi-continuous cylindrical reactor with the internal volume of 1500 mL was assembled for the catalytic ozonation of the wastewater (Fig. 1). Using this reactor, ozone could continuously be bubbled into the wastewater. The off-gas containing the excess ozone could then be directed from the reactor to gas scrubbers containing 20% potassium iodide where the excess ozone could be decomposed.

The catalytic ozonation experiments were conducted at room temperature using 50 mL of the wastewater samples mixed with 450 mL double distilled water and 0.3 mg MgO nanoparticles. The pH was adjusted at various values of 3, 5, 7 and 9 employing 0.1 M solutions of HCl or NaOH. For a typical experiment, the solution was transported into the glass reactor shown in Fig. 1, connected to a DONALIO3 ozone generator with an ozone production capacity of 0.2 g/h, and treated for 10, 20, and 30 min. After specific periods, the quantity of remaining benzene, toluene, ethylbenzene, and xylene present in the wastewater samples were measured by injecting 1 μL of the sample into the GC equipment.

Simple ozonation process (SOP) and adsorption process (AP)

In addition to the COP, SOP and AP were also evaluated using petrochemical wastewater samples in order to distinguish the effect of various phenomena which could be involved in the removal, or the reduction, of contaminants present in the wastewater. To perform the SOP, 50 mL of the wastewater was mixed with 450 mL of double distilled water at different pH values of 3, 5, 7 and 9. For this, the pH of wastewater was adjusted with solutions containing 0.1 N of HCl or NaOH. Then, the ozonation process was carried out at reaction durations of 10, 20, and 30 min to evaluate the influence of time on the process.

The AP was performed under the same conditions as mentioned above for SOP, with the difference that no ozone was involved, and instead, around of 0.3 mg MgO nanoparticles was added to the wastewater. Moreover, the solution was aerated to create turbulence in order to achieve an appropriate contact between the solution and MgO nanoparticles.

At the end of both processes, the samples were rested for 5 min, and 5 mL aliquots were collected from the middle level of the reactor, from which 1 μL samples were injected into the GC instrument for determining the quantities of contaminants remaining in the solution.

Results and Discussion

Characterization of MgO nanocatalysts

The SEM surface morphology of MgO nanoparticles is shown in Fig. 2a, from which the presence of spherical shaped and agglomerated particles is evident. TEM image of the material (Fig. 2b) clearly indicates that individual MgO nanoparticles have an average dimension of around 30 nm. X-ray diffraction pattern of MgO nanoparticles, presented in Fig. 2c, indicate the reflections at 2θ = 37°, 43°, 62°, 74°, and 78° corresponding to (111), (200), (220), (311), and (222) characteristic XRD peaks of MgO with a cubic structure (JCPDS 01-075-1525), respectively. Scherrer equation can be employed to evaluate the size of crystals in ceramic materials [33–35]. The mean crystallite size of MgO nanoparticles could be calculated using this approach, based on the most intense (002) XRD peak observed in Fig. 2c, and found to be around 21 nm. This is in agreement with the nanostructured nature of the material.

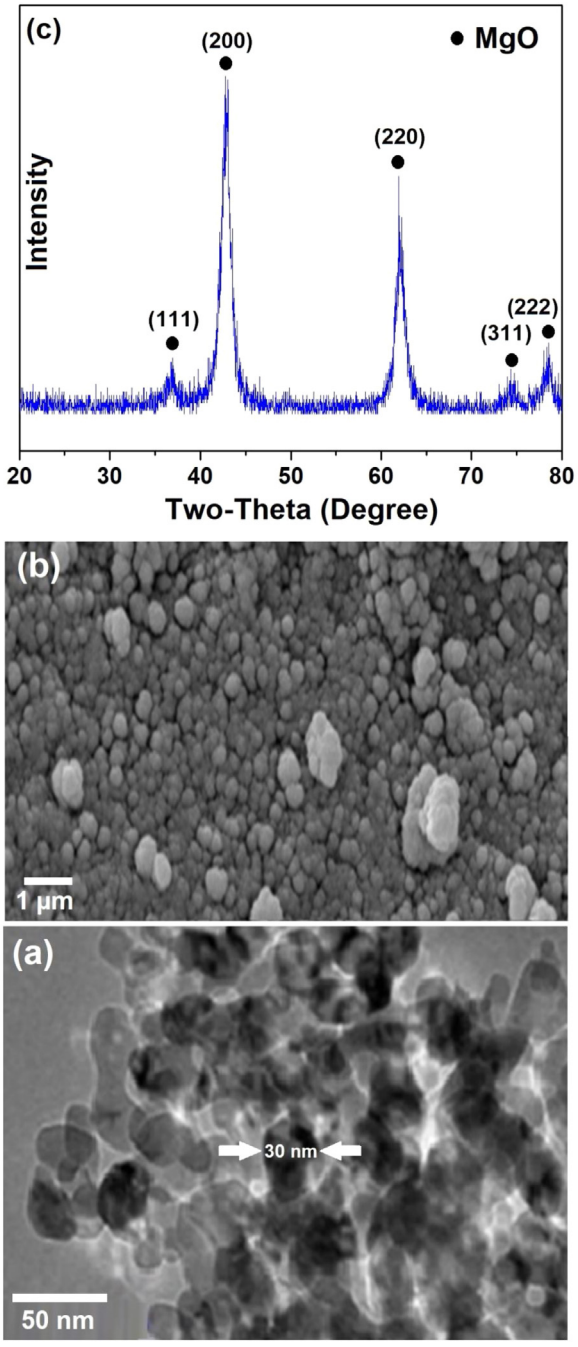

Fig. 2 – (a) SEM, (b) TEM, and (c) XRD analysis of MgO nanoparticles synthesized using the calcination method.

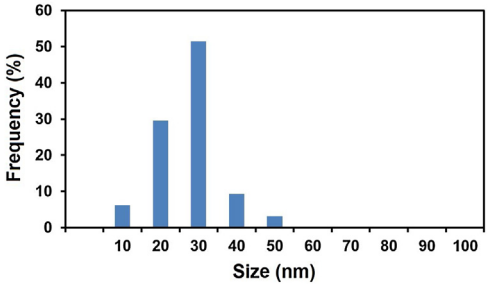

Fig. 3 – The particle size distribution histogram of MgO nanoparticles.

It should be mentioned that there are several techniques to prepare ceramic nanoparticles including hydrothermal methods [36,37], sol-gel [38,39], spark discharge [40], electrochemical discharge machining [41], laser ablation [43,43], ball milling [44], aqueous wet chemical method [45], combustion synthesis [46–49] and molten salt-based techniques [50–53]. Comparing to these techniques, the simple calcination method used in this study for the preparation of MgO nanoparticles (reaction (1)) may benefit from relative simplicity, low cost and minimal requirement for complex equipment.

$Mg(NO_3)_2 = MgO + 2NO_2(g) + 1/2O_2(g)\ \Delta G^{\circ}{}_{500\,^{\circ}C} = -80\,kJ$ (1)

It should be mentioned that NO_2 produced as the by-product of the reaction (1) can be used in the manufacturing of nitric acid by treating with water and air [54–56], improving the economic performance of the process. It is worth noticing that the demand for nitric acid is considerably increasing due to its wide range of applications, including in the processing of fertiliser, mining explosives and gold extraction [57]. The surface area of the MgO nanoparticles produced in our study was measured by N_2 adsorption/desorption measurements (TriStar II 3020 Micromeritics) and found to be 221 m^2/g, with BJH Adsorption cumulative pores volume of 0.85 cm3/g, and BJH adsorption average pore diameter of 27.4 nm.

Fig. 3 shows the particle size distribution histogram of MgO nanoparticles calculated from TEM analysis, which was built up by counting more than 100 particles. From this, an average diameter of 22.6 nm can be obtained. We can compare this value with those presented in the literature. Wong et al. [58] prepared MgO nanoparticles employing an ultra-sonication incorporated Pechini method [59] using magnesium acetate tetrahydrate and citric acid as the raw materials. The value of average size of MgO nanoparticles produced under different conditions were measured to be around 21 -122 nm. In another work, Hajengia et al. [60] produced MgO nanoparticles with an average particle size of 16 nm by the microwave heating of a mixture comprising $Mg(CH_3COO)_2{\cdot}4H_2O$ and benzylamine to form $Mg(OH)_2$ which was separated, washed and calcined at 550 °C for 5 h. The particle size distribution histogram of the sample demonstrated that the most of the particles were in the range of 12–22 nm. Furthermore, Kumar et al. [61] produced MgO nanostructures with particle size of 20-25 nm by a combustion route using $Mg(NO_3)_2\ .6H_2O$ as the magnesium source and vetiver as the fuel. Overall, the characteristics of MgO nanoparticles produced in this study by a simple calcination technique are compatible with those produced by alternative, generally more complicated/expensive techniques.

The effect of variation time of wastewater treatment

The effects of time variation on the efficiency of COP, SOP and AP to remove chemicals from the petrochemical wastewater are exhibited in Fig. 4a-c. As can be depicted from Fig. 4a, the benzene removal efficiency in the SOP improved from 9% to 33% when the reaction time increased from 10 to 30 min. At this time slot, the improvement in the removal efficiency of toluene, ethylbenzene, and xylene could be recorded to be 18

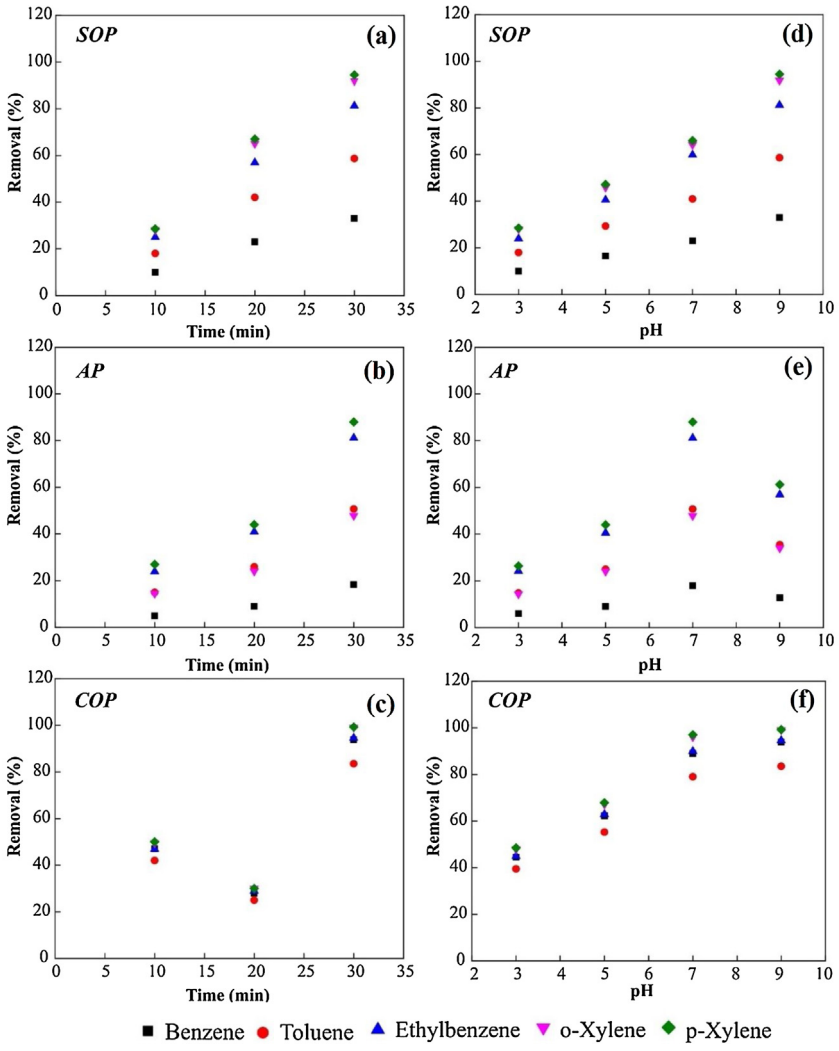

Fig. 4 – Influence of the variation of time and pH on the performance of SOP, AP and COP for the removal of contaminates from the petrochemical wastewater. The variation of reaction durations at the pH value of 7.5 (Table 1) for (a) SOP, (b) AP, and (c) COP. The variation of the pH solution at the contact time of 30 min for (d) SOP, (e) AP, and (f) COP.

to 58%, 25 to 81%, and 28 to 92%, respectively. Likewise, in the AP, the increase in reaction time from 10 to 30 min improved the benzene removal efficiency from 5 to 18%. For toluene, ethylbenzene, and xylene, the improvement in the removal efficiency was measured to be 15 to 50%, 24 to 81%, and 27 to 88%, respectively (Fig. 4b). As shown in Fig. 4c, the removal efficiency in the COP for benzene rose from 47 to 93% when the reaction time increased from 10 to 30 min. The improvement recorded for the removal efficiencies of toluene, ethylbenzene, and xylene was from 42 to 83%, 47 to 94%, and 50 to more than 99%, respectively. The COP procedure presents the highest efficient of removal for all contaminants, denoting the positive influence of the catalytic process promoted by MgO nanoparticles.

The effect of pH on the wastewater treatment efficiency

Since pH is an important factor in ozonation process, its effect on the efficiency of SOP, AP and CPO for the removal of various contaminants from the petrochemical wastewater was evaluated, and the results can be observed in Figs. 4d-f. As shown in Fig. 4d, the removal efficiency increases in the SOP by increasing the pH value. For p-Xylene, the removal efficiency increased from about 28% at pH 3 to 94.5% at pH 9. As shown in Fig. 4e, in the AP, the adsorption efficiencies of MgO nanoparticles for all the chemicals increase when the pH increases to about the neutral value, but considerably decline by further increasing the pH value to 9. As presented in Fig. 4f, in the COP, the efficiencies for the removal of chemicals increase by increasing the pH values. For instance, the removal efficiency of ethylene, benzene and xylene increased from 45-50% at pH 3 to more than 90% at pH 9. As presented in Fig. 4f, by increasing the pH level of the solutions from 3-9, the efficiency of COP process to remove various contaminants from the petrochemical wastewater increases. It is noteworthy that more than 90 percent of all the petroleum compounds present in the wastewater could be decomposed at pH = 9 after 30 min of treatment. It should be noticed that the positive relation of pH

with SOP efficiency to degraded organic compounds was also previously observed [23]. Such a relation can also be indicated for the case of COP as evident in Fig. 4f.

Results obtained indicate that the duration of ozonation and contact time enhance the overall performance of SOP, AP and COP. The highest removal efficiencies achieved can be summarized as 94.5, 88, and 99.2% for the SOP, the AP, and COP, respectively, obtained after 30 min of treatments. Therefore, the order of removal efficiency of organic pollutants can be regulated as AP < SOP < COP.

The adsorption proprieties and catalytic performance of MgO for the degradation of n-alkanes have been evaluated in the literature [62,63], highlighting the electron-acceptor and electron-donor abilities of the MgO surface. Those studies identify that the dye adsorption performance of MgO nanoparticles is maximized at the pH value of 6, which is in an approximate agreement with our results obtained for AP presented in Fig. 4e.

For the case of COP, the removal efficiencies are approximately same at the pH values of 7 and 9, providing the maximum pollutants degradation performances. This results is in agreement with those obtained by Moussavi et al. [64].

These authors suggested a mechanism for the degradation of phenol by COP, based on which, in the presence of ozone, the Lewis acid sites on the surfaces of MgO particles (MgO-s) react with ozone, and eventually with phenol, leading to the degradation event. This mechanism may also shed light on the degradation of pollutants in the current study, as explained by the occurrence of reactions (1)-(4).

$O_3 + MgO\text{-}s \rightarrow MgO\text{-}s^{O3}$ (1)

$MgO\text{-}s^{O3} \rightarrow MgO\text{-}s^{O\bullet} + O_2$ (2)

$MgO\text{-}s^{O\bullet} + pollutant \rightarrow CO_2 + H_2O + intermediates$ (3)

$MgO + pollutant + O_3 \rightarrow CO_2 + H_2O + intermediates$ (4)

Reaction (4) can be regarded as the direct oxidation of pollutant with O_3 molecules.

On the other hand, regarding the degradation of organic molecules in the presence of O_3 as an oxidizer ($E^0 = +2.07$ eV), it is known that under alkaline conditions, the decomposition of O_3 molecules occurs with the production of hydroxyl radicals (•OH) [65]. These radicals have an even greater oxidative potential (E0 = + 2.8 eV) for decomposition of organic molecules [66,67].

In the presence of a catalyst, the production of •OH can be stimulated. Also, the increase in the pH value of the reaction medium can accelerate the mass transfer of O_3 and its decomposition rate, promoting the formation of highly reactive free radicals, such as •OH, $\bullet O_2H$ and $\bullet O_3H$, leading to the increase of pollutants degradation efficiency [32,68,69].

The formation of $^{\bullet}$OH and MgO-hydroxyl ($MgO\text{-}s^{OH}$) radicals have been explained to occur based on reactions (5) and (6) [32].

$MgO\text{-}s^{O\bullet} + 2H_2O + O_3 \rightarrow MgO\text{-}s^{OH} + 3\ \bullet OH + O_2$ (5)

$\bullet OH + O_2 + pollutant \rightarrow CO_2 + O_2^- + H_2O$ (6)

The $^{\bullet}$OH radicals could also be produced in COP, providing a more effective environment for the oxidation of organic pollutants present in the petrochemical wastewater, in comparison with radicals produced by SOP. The reactions (3), (4) and (6) can occurs simultaneously, improving the overall degradation efficiency.

Treatment of the petrochemical wastewater at the pH value of 12

Inspired by the experimental results, the petrochemical wastewater was further treated using the three distinct approaches; SOP, AP and COP, to reduce its contamination level under deviated conditions from those exhibited in Fig. 4, i.e. the enhanced pH value of 12, and extended contact duration of 50 min. The results obtained are presented in Fig. 5. As indicated, in the SOP, the xylene removal percentage is higher compared to that of ethylene benzene, toluene, and benzene. Moreover, the removal percentage of xylene and ethylbenzene in the AP are very close to each other and both higher than those of benzene and toluene. The lowest removal efficiency is related to that of benzene (33%). These observations can be explained by the combination of effects, comprising the lower solubility of benzene and toluene compared to ethylbenzene and xylene, and the higher molecular weights and melting points of xylene and ethylbenzene compared to benzene and toluene [70–72].

As shown in Fig. 5, in the AP, the highest and lowest (18%) removal efficiency could be achieved for p-Xylene and benzene, respectively. Moreover, the removal percentage of o-Xylene is lower than those of ethylbenzene and paraxylene.

As indicated by Lu et al. [72], at the initial benzene and toluene concentrations of 60 and 200 mg/L, respectively, toluene adsorption per unit of the adsorbent mass was greater than that of benzene. Moreover, Aivalioti et al. [70] showed that the adsorption capacity of diatomic adsorbents was higher for toluene than benzene. Yakout and Daifullah [73] found that a higher amount of toluene could be adsorbed per unit mass of the activated carbon than benzene. Furthermore, Su et al. [74] showed that the capacity of carbon nanotubes modified by sodium hypochlorite for the adsorption of benzene and toluene are 212 and 225 mg/g of the adsorbent, respectively, at their initial concentration of 200 mg/L, the contact time of 240 min, and adsorbent concentration of 600 mg/L. Other studies show that activated carbon adsorbent could reduce petroleum contaminants from water by up to 80% [75], although it cannot completely remove organic matter from water. Garoma et al. [76] found that the removal efficiencies of petroleum compounds by SOP could be 27%. Furthermore, they noticed that SOP was more efficient than the AP using MgO nanoparticles in removing contaminants, except for ethylbenzene, for which SOP and the AP exhibited almost the same efficiency.

As mentioned earlier, it should be noticed that molecular ozone has a high oxidation-reduction potential of 2.07 V vs. SHE, which is greater than those of most oxidants such as chlorine (1.48 V), but lower than that of hydroxyl radicals (2.8 V) [77]. As shown in Fig. 5, the COP is much more efficient than the SOP and the AP. The reason for this might lie in the fact that the simultaneous use of ozone and adsorbent accelerates the transformation of ozone from its molecular state into hydroxyl radicals. This is in agreement with the work of Dehouli et al. [78], who found that the utilization of ozonation together with the activated carbon could enhance the wastewater treatment performance, and this was attributed to the greater quantities of hydroxyl radicals present in the COP.

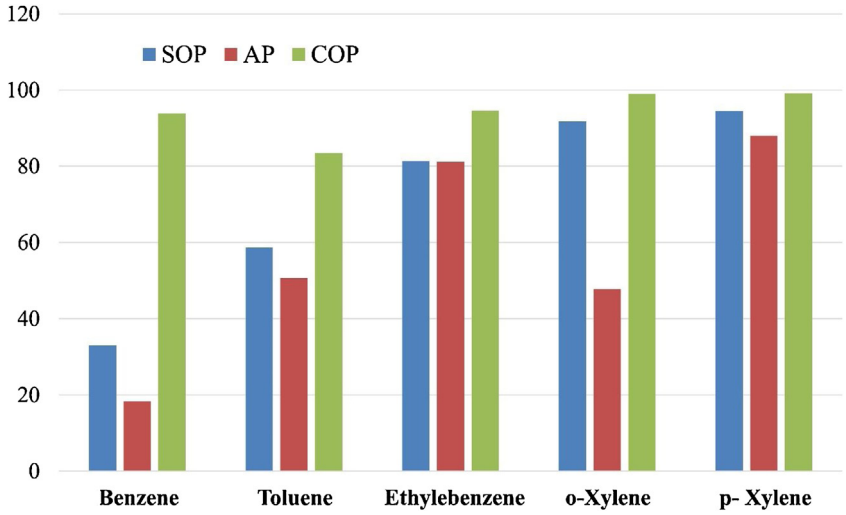

Fig. 5 – The efficiency of SOP, AP and COP for the removal of various chemicals from the petrochemical wastewater, after 50 min of the treatment at the pH level of 12.

Table 2 – A summary on the performance of various techniques used for the removal of contaminants from the petrochemical wastewater: Concentrations of poullants in the raw wastewater (CR), and those after the ozonation (CO), the adsorption (C-AP), and the catalytic ozonation (C-COP). The removal efficiency in the ozonation process (E-SOP), adsorption (E-AP), and the catalytic ozonation (C-COP).

Pollutant	CR	CO	C-AP	C-COP	E-SOP	E-AP	E-COP
Benzene	510.7	341.2	417.1	31.2	33%	18.3%	93.8%
Toluene	725	298.9	357	119.5	58.7%	50.7%	83.5%
Ethylbenzene	436.9	81.3	82	23.4	81.3%	81.2%	94.6%
o-Xylene	497.2	40.3	259.3	2.4	91.8%	47.8%	99%
p-Xylene	341.4	18.6	40.4	6.2	94.5%	88%	99.2%

The performance of COP for the removal of Reactive Red 198 in the presence MgO nanocrystals was found to be related to the decomposition of dye molecules due to indirect oxidation by the active radicals [32]. Valdez et al. [79,80] examined the effects of COP together with volcanic rocks in the benzothiazole removal, and related the high efficiency of the process to the intense inclination of ozone to react with Lewis acids of the metal oxides in the volcanic rocks. Moreover, results indicated that the COP performed better than the SOP at contact time of 30 min. Since both direct and indirect oxidations are involved in contaminant removal in the COP, the process exhibits a higher performance at shorter contact periods compared to the common SOP. It should also be noticed the ozone decomposition can be enhanced on the adsorbent surfaces results in higher concentrations of the free radicals in the system, promoting the decomposition of organic pollutants [80].

It has been found that ozone decomposition can be promoted on the surfaces of crystals of natural zeolite, and particularly on volcanic rocks [79–81]. It was because such materials are capable of adsorbing ozone, followed by its conversion into free radicals.

From Figs. 4 and 5, the enhanced performance of the heterogeneous COP process, comparing to SOP and AP is evident. The catalyst surface properties, therefore, play an important role in the ozonation process, as also indicated by Zhang et al. [82]. Based on the results obtained by Mohammadi et al. [29], COP is an efficient and rapid method for removing of toluene from aqueous solutions. It is known that metal oxides are able to adsorb water molecules, and this causes the formation of surface hydroxyl groups. Such hydroxyl groups exhibit various electric charge patterns at different pH values [83], affecting the decomposition of ozone on the metal oxide's surface. For instance, Qi et al. [84] studied the degradation of 2, 4, 6-trichloroanisole by the ozonation process in the presence of Al_2O_3 particles, and found that the decomposition of ozone on the alumina particles is enhanced when pH level approaches around 8. Furthemore, Garoma et al. [76] concluded that in ozonation experiments, the presence of sufficient amount of iron in groundwater samples would improve the removal of BTEX, MTBE, TBA, and TPHg. These observations are in agreement with our experimental results. Table 2 summarizes the performance of the SOP, AP and COP processes for the removal of the pollutants from the petrochemical wastewater.

It is known that the physical and chemical properties of contaminants significantly influence their removal performance from wastewaters [85].

For instance, in advanced oxidation treatments, xylene can be eliminated more than chemicals such as ethylbenzene, toluene, and benzene. Furthermore, the amount of adsorbed ethylbenzene and xylene is very close, whilst their adsorption values are considerably higher than those of benzene and toluene. These characteristics can be explained based on the properties of these chemicals. Based on this, the relatively high dissolution rate of benzene in water (1780 ppm) in

comparison to other compounds such as toluene (512 ppm), ethyl benzene (152 ppm), and xylene (175 ppm) [86,87], makes it more difficult to be removed from wastewasters. The considerably higher molecular weight and boiling points of xylene and ethylbenzene than toluene and benzene around (around 144, 136, 111, and 80 °C, respectively) can also influence their removal efficiency [70,88].

Remarks and conclusions

Petroleum-derived chemicals can be hazardous and toxic threatening the human health and environment security. These compounds may enter the food chain via various routes, one of which is the water resources. Therefore, the removal of petrochemical contaminants from water resources is of significant importance. This can be carried out by various methods, including adsorption and ozonation; considering that each technique has its own advantages and disadvantages. Catalytic oxidation processes are among promising water treatment methods which have the advantages of both adsorption and oxidation approaches. Here, we investigated the performance of AP, SOP, and COP on the removal of various contaminants (benzene, toluene, ethylbenzene, and xylene) from petrochemical wastewaters, collected from an Iranian petrochemical industry. MgO nanoparticles produced by the calcination of Mg $(NO_3)_2 6H_2O$ with a mean particle size of around 23 nm was used as the catalyst. The effects of contact time and pH were evaluated for each approach. Results showed the considerably higher performance of COP in comparison with those of SOP and AP. The increase in the contact time and the pH value of the solutions led to the improvement of removal efficiencies. During 30 min of the COP, the removal efficiencies of benzene, toluene, ethylbenzene, and xylene were recorded to be 93, 83, 94, and 99.2%; which are considerably greater than those obtained in SOP; 33, 58, 81, and 92%, respectively. MgO-enhanced COP can be considered a promising and economical approach for the removal of petroleum-based pollutants from aqueous environments.

Declaration of interests

The authors declare that they have no known competing financial interests or personal relationships that could have appeared to influence the work reported in this paper.

The authors declare the following financial interests/personal relationships which may be considered as potential competing interests:

Uncited reference

[42].

REFERENCES

[1] C.K. Thompson, C.P. Nathanail, The risk assessor as the customer in: Chemical Analysis of Contaminated Land, CRC Press, Oxford, 2003, pp. 1–19.

[2] A.M.A. Pintor, V.J.P. Vilar, C.M.S. Botelho, R.A.R. Boaventura, Oil and grease removal from wastewaters: Sorption treatment as an alternative to state-of-the-art technologies, A critical review, Chem. Eng. J. 297 (2016) 229–255.

[3] M.H. Al-Malack, Treatment of petroleum refinery wastewater using crossflow and immersed membrane processes, Desalin, Water Treat. 51 (2013) 6985–6993.

[4] N.S. Mizzouri, M.G. Shaaban, Individual and combined effects of organic, toxic, and hydraulic shocks on sequencing batch reactor in treating petroleum refinery wastewater, J. hazard, Mater. 15 (2013) 333–344.

[5] J. Zhong, X. Sun, C. Wang, Treatment of oily wastewater produced from refinery processes using flocculation and ceramic membrane filtration, Sep. Purif. Technol. 32 (2003) 93–98.

[6] S. Ishak, A.M. Malakahmad,.H. Isa, Refinery wastewater biological treatment: A short review, J. Sci. Ind. Res. 71 (2012) 251–256.

[7] M.M. Rahman, M.H. Al-Malack, Performance of a crossflow membrane bioreactor (CF–MBR) when treating refinery wastewater, Desalination 191 (2006) 16–26.

[8] S. Malmasi, S.A. Jozi, S.M. Monavari, M.E. Jafarian, Ecological impact analysis on Mahshahr petrochemical industries using analytic hierarchy process method, Int. J. Environ. Res. 4 (2010) 725–734.

[9] X.P. Jia, F.Y. Han, X.S. Tan, Integrated environmental performance assessment of chemical processes, Comput. Chem. Eng. 29 (2004) 243–247.

[10] R. Seth, E.K. Tam, Toxic impact assessment of a manufacturing process: illustrative application to the automotive paint process, Int. J. Environ. Stud. 63 (2006) 453–462.

[11] S.G. Won, S.A. Baldwin, A.K. Lau, M. Rezadehbashi, Optimal operational conditions for biohydrogen production from sugar refinery wastewater in an ASBR, Int. J. Hydrogen energy 38 (2013) 13895–13906.

[12] M.H. El-Naas, M.A. Alhaija, S. Al-Zuhair, Evaluation of a three-step process for the treatment of petroleum refinery wastewater, J. Environ. Chem. Eng. 2 (2014) 56–62.

[13] P. Stepnowski, E.M. Siedlecka, P. Behrend, B. Jastorff, Enhanced photo-degradation of contaminants in petroleum refinery wastewater, Water Res. 36 (2002) 2167–2172.

[14] M. Sánchez-Polo, U. von Gunten, J. Rivera-Utrilla, Efficiency of activated carbon to transform ozone into OH radicals: influence of operational parameters, Water Res. 39 (2005) 3189–3198.

[15] T.A. Kurniawan, W.H. Lo, G.Y. Chan, Degradation of recalcitrant compounds from stabilized landfill leachate using a combination of ozone-GAC adsorption treatment, J. Hazard. Mater. 137 (2006) 443–455.

[16] J.C. Kruithof, P.C. Kamp, B.J. Martijn, UV/H2O2 treatment: a practical solution for organic contaminant control and primary disinfection, Ozone Sci. Eng. 29 (2007) 273–280.

[17] E.J. Rosenfeldt, K.G. Linden, S. Canonica, U. Von Gunten, Comparison of the efficiency of OH radical formation during ozonation and the advanced oxidation processes O3/H2O2 and UV/H2O2, Water Res. 40 (2006) 3695–3704.

[18] L. Labiadh, S. Ammar, A.R. Kamali, Oxidation/mineralization of AO7 by electro-Fenton process using chalcopyrite as the heterogeneous source of iron and copper catalysts with enhanced degradation activity and reusability, J. Electroanal. Chem. 853 (2019) 113532.

[19] G. Tchobanoglous, F. Burton, Wastewater engineering: Treatment disposal reuse, McGraw-Hill Inc, 1990.

[20] I. Michael, E. Hapeshi, C. Michael, A.R. Varela, S. Kyriakou, C.M. Manaia, D. Fatta-Kassinos, Solar photo-Fenton process on the abatement of antibiotics at a pilot scale: degradation kinetics, ecotoxicity and phytotoxicity assessment and

removal of antibiotic resistant enterococci, Water Res. 46 (2012) 5621–5634.
[21] R. Anjali, S. Shanthakumar, Insights on the current status of occurrence and removal of antibiotics in wastewater by advanced oxidation processes, J. Environ. Manag. 246 (2019) 51–62.
[22] F. Ingerslev, L. Toräng, M.L. Loke, B. Halling-Sørensen, N. Nyholm, Primary biodegradation of veterinary antibiotics in aerobic and anaerobic surface water simulation systems, Chemosphere 44 (2001) 865–872.
[23] A. Lv, C. Hu, Y.J. Nie, Qu Catalytic ozonation of toxic pollutants over magnetic cobalt and manganese co-doped γ-Fe2O3, Appl. Catalysis B Environ. 100 (2010) 62–67.
[24] J. Nawrocki, B. Kasprzyk-Hordern, The efficiency and mechanisms of catalytic ozonation, Appl., Catalysis B Environ 99 (2010) 27–42.
[25] H. Valdés, V.J. Farfán, J.A. Manoli, C.A. Zaror, Catalytic ozone aqueous decomposition promoted by natural zeolite and volcanic sand, J. Hazard. Mater. 165 (2009) 915–922.
[26] Y. Haldorai, J.J. Shim, An efficient removal of methyl orange dye from aqueous solution by adsorption onto chitosan/MgO composite: A novel reusable adsorbent, Appl. Surf. Sci. 292 (2014) 447–453.
[27] X. Zheng, K. Wang, Z. Huang, Y. Liu, J. Wen, H. Peng, MgO nanosheets with N-doped carbon coating for the efficient visible-light photocatalysis, J. Ind. Eng. Chem. 76 (2019) 288–295.
[28] E. Vesali-Kermani, A. Habibi-Yangjeh, S. Ghosh, Visible-light-induced nitrogen photofixation ability of g-C3N4 nanosheets decorated with MgO nanoparticles, J. Ind. Eng. Chem. 84 (2020) 185–195.
[29] L. Mohammadi, E. Bazrafshan, M. Noroozifar, A. Ansari-Moghaddam, Application of heterogeneous catalytic ozonation process with magnesium oxide nanoparticles for Toluene degradation in aqueous environments, Health Scope 5 (2016) 40439.
[30] G. Asgari, J. Faradmal, H. Zolghadr Nasab, H. Ehsani, Catalytic ozonation of industrial textile wastewater using modified C-doped MgO eggshell membrane powder, Adv. Powder Technol. 30 (2019) 1297–1311.
[31] J.E. Lee, B.S. Jin, S.H. Cho, S.H. Han, O.S. Joo, K.D. Jung, Catalytic ozonation of humic acids with Fe/MgO, Korean J. Chem. Eng. 22 (2005) 536–540.
[32] G. Moussavi, M. Mahmoudi, Degradation and biodegradability improvement of the reactive red 198 azo dye using catalytic ozonation with MgO nanocrystals, Chem. Eng. J. 152 (2009) 1–7.
[33] A.R. Kamali, D.J. Fray, Preparation of lithium niobate particles via reactive molten salt synthesis method, Ceram. Int. 40 (2014) 1835–1841.
[34] A.R. Kamali, D.J. Fray, Solid phase growth of tin oxide nanostructures, Mater. Sci. Eng. B 177 (2012) 819–825.
[35] A.R. Kamali, Nanocatalytic conversion of CO2 into nanodiamonds, Carbon 123 (2017) 205–215.
[36] Z.X. Tang, Bin-Feng Lv MgO nanoparticles as antibacterial agent: preparation and activity, Brazilian J. Chem. Eng 31 (2014) 591–601.
[37] W.N. Abdel Aziz, A. Bumajdad, F. Al Sagheer, M. Madkour, Selective synthesis and characterization of iron oxide nanoparticles via PVA/PVP polymer blend as structure-directing agent, Mater. Chem. Phys. 249 (2020) 122927.
[38] L. Zhu, M. Awais, H. Muhammad, A. Javed, M. Salman, M. Tlilief, S. Ullah Khan, M. Shadloo, Photo-catalytic pretreatment of biomass for anaerobic digestion using visible light and Nickle oxide (NiOx) nanoparticles prepared by sol gel method, Renew. Energy 154 (2020) 128–135.
[39] M. Parashar, V. Kumar Shukl, R. Singh, Metal oxides nanoparticles via sol–gel method: a review on synthesis, characterization and applications, J, Mater. Sci. Mater. El. 31 (2020) 3729–3749.
[40] T. Němec, J. Šonský, J. Gruber, E. Prado, J. Kupčík, M. Klementová, Platinum and platinum oxide nanoparticles generated by unipolar spark discharge, J. Aerosol Sci. 141 (2020) 10550.
[41] H. Bishwakarma, A. Kumar Das, Synthesis of zinc oxide nanoparticles through hybrid machining process and their application in supercapacitors, J. Electron. Mater. 49 (2020) 1541–1549.
[42] M. Fernández-Arias, M. Boutinguiza, J. del Val, A. Riveiro, D. Rodríguez, F. Arias-González, J. Gil, J. Pou, Fabrication and deposition of copper and copper oxide nanoparticles by laser ablation in open air, Nanomaterials 10 (2020) 300.
[43] E. Naseri, G. Dorranian, A.H. Sari, Characterization of cobalt oxide nanoparticles produced by laser ablation method: Effects of laser fluence, Physica E Low Dimens. Syst. Nanostruct. 115 (2020) 113670.
[44] J. Singh, S. Sharma, S. Soni, S. Sharma, R.C. Singh, Influence of different milling media on structural, morphological and optical properties of the ZnO nanoparticles synthesized by ball milling process, Mater, Sci. Semicond. Process. 98 (2019) 29–38.
[45] F. Khairallah, A. Glisenti, Synthesis, characterization and reactivity study of nanoscale magnesium oxide, J, Mol. Catal. A Chem. 274 (2007) 137–147.
[46] N. Javadi, B. Arghavan, V. Saghir, S.M. Beidokhti, J. Vahdati Khaki, Modified auto-combustion synthesis of mixed-oxides TiO2/NiO nanoparticles: Physical properties and photocatalytic performance, Ceram. Int. 46 (2020) 15417–15437.
[47] H. Aliasghari, A.M. Arabi, H. Haratizadeh, A novel approach for solution combustion synthesis of tungsten oxide nanoparticles for photocatalytic and electrochromic applications, Ceram. Int. 46 (2020) 403–414.
[48] A.R. Kamali, S.H. Shishavan, M.N. Samani, A. Rezaei, K.B. Kim, Ultra-fast shock-wave combustion synthesis of nanostructured silicon from sand with excellent Li storage performance, Sustain. Energy Fuels 3 (2019) 1396–1405.
[49] A.R. Kamali, H. Razavizadeh, S.M.M. Hadavi, A new process for titanium aluminides production from TiO2, J. Mater. Sci.Technol. 23 (2007) 367–372.
[50] A.R. Kamali, G. Divitini, C. Ducati, D.J. Fray, Transformation of molten SnCl2 to SnO2 nano-single crystals, Ceram. Int. 40 (2014) 8533–8538.
[51] A.R. Kamali, Thermokinetic characterisation of tin(II) chloride, J. Therm. Anal. Calorim. 118 (2014) 99–104.
[52] W. Zhu, A.R. Kamali, Green molten salt synthesis and Li-ion storage performance of sodium dimolybdate, J. Alloys Compd. 831 (2020) 15478.
[53] A.R. Kamali, J. Feighan, D.J. Fray, Towards large scale preparation of graphene in molten salts and its use in the fabrication of highly toughened alumina ceramics, Faraday Discuss. 190 (2016) 451–470.
[54] C. Anastasi, P.P. Bemand, I.W.M. Smith, Rate constants for: OH + NO2 (+ N2) → HNO3 (+ N2) between 220 and 358 K, Chem. Phys. Lett. 37 (1976) 370–372.
[55] A.R. Salman, B.C. Enger, X. Auvray, R. Lødeng, M. Menon, D. Waller, M. Rønning, Catalytic oxidation of NO to NO2 for nitric acid production over a Pt/Al2O3 catalyst, Appl. Catal. A 564 (2018) 142–146.
[56] J. Li, X. Han, X. Zhang, A.M. Sheveleva, Y. Cheng, F. Tuna, E.J.L. McInnes, L.J.M. McPherson, S.J. Teat, L.L. Daemen, A.J.R. Cuesta, M. Schröder, S. Yang, Capture of nitrogen dioxide and conversion to nitric acid in a porous metal–organic framework, Nature Chem. 11 (2019) 1085–1090.

[57] H. Frankland, C. Brown, H. Goddin, O. Kay, T. Bünnagel, One hundred years of gauze innovation, Johnson Matthey Tech. Rev. 61 (2017) 183–189.
[58] C.W. Wong, Y.S. Chan, J. Jeevanandam, K. Pal, M. Bechelany, M.A. Elkodous, G.S. El-Sayya, Response surface methodology optimization of mono-dispersed MgO nanoparticles fabricated by ultrasonic-assisted sol–gel method for outstanding antimicrobial and antibiofilm activities, J. Cluster Sci. 31 (2020) 367–389.
[59] C. Yerlikaya1, N. Ullah, A.R. Kamali, R.V. Kumar, Size-controllable synthesis of lithium niobate nanocrystals using modified Pechini polymeric precursor method, J. Therm. Anal. Calorim. 125 (2016) 17–22.
[60] A.L. Gajengia, T. Sasakib, B.M. Bhanag, Mechanistic aspects of formation of MgO nanoparticles under microwave irradiation and its catalytic application, Adv. Powder Technol. 28 (2017) 1185–1192.
[61] N.B. Arun Kumar, B. Mahendra, J. Sirajudeeen, M.R. Anil Kumar, H.P. Nagaswarupa, C.R. Ravi, K.B. Umesh, Green mediated synthesis of MgO nano-flakes and its electro-chemical applications, Mater. Today: Proceedings 5 (2018) 22275–32228.
[62] T.G. Venkatesha, R. Viswanatha, Y. Arthoba Nayaka, B.K. Chethana, Kinetics and thermodynamics of reactive and vat dyes adsorption on MgO nanoparticles, Chem. Eng. J. 198–199 (2012) 1–10.
[63] S.N. Lanin, N.V. Kovaleva, K.S. Pham Tien Dung, Lanina, Adsorption properties and surface chemistry of MgO, Mosc. Univ. Chem. Bull. 63 (2008) 250–254.
[64] G. Moussavi, A. khavanin, R. Alizadeh, The integration of ozonation catalyzed with MgO nanocrystals and the biodegradation for the removal of phenol from saline wastewater, Appl. Catal. B: Environ. 97 (2010) 160–167.
[65] K. He, Y.M. Dong, Z. Li, L. Yin, A.M. Zhang, Y.C. Zheng, Catalytic ozonation of phenol in water with natural brucite and magnesia, J. Hazard. Mater. 159 (2008) 587–592.
[66] H. Xiao, Y. Xu, M. Yu, Q. Zhang, Enhanced mineralization of 2 4-dichlorophenol by ozone in the presence of trace permanganate: effect of pH, Environ Technol. 31 (2010) 1295–1300.
[67] W.B. Wang, H. Zhang, F. Wang, X. Xiong, K. Tian, Y. Sun, T. Yu, Application of Heterogeneous Catalytic Ozonation for Refractory Organics in wastewater, Catalysts 9 (2019) 241.
[68] H. Yan, P. Lu, Z. Pan, X. Wang, Q. Zhang, L. Li, Ce/SBA-15 as a heterogeneous ozonation catalyst for efficient mineralization of dimethyl phthalate, J Molecular Catalysis A: Chem. 377 (2013) 57–64.
[69] H. Yan, W. Chen, G. Liao, X. Li, S. Ma, L. Li, Activity assessment of direct synthesized Fe-SBA-15 for catalytic ozonation of oxalic acid, Sep. Purif. Technol. 159 (2016) 1–6.
[70] M. Aivalioti, I. Vamvasakis, E. Gidarakos, BTEX and MTBE adsorption onto raw and thermally modified diatomite, J. Hazard. Mater. 178 (2010) 136–143.
[71] H.T. Gomes, P.V. Samant, P. Serp, P. Kalck, J.L. Figueiredo, J.L. Faria, Carbon nanotubes and xerogels as supports of well-dispersed Pt catalysts for environmental applications, Appl. Catalysis B Environ. 54 (2004) 175–182.
[72] C. Lu, F. Su, S. Hu, Surface modification of carbon nanotubes for enhancing BTEX adsorption from aqueous solutions, Appl. Surf. Sci. 254 (2008) 7035–7041.
[73] S.M. Yakout, A.A.M. Daifullah, Adsorption of toluene, ethylbenzene and xylenes by activated carbon-impact of molecular oxygen, Desalin, Water Treat. 52 (2014) 4977–4981.
[74] F. Su, C. Lu, S. Hu, Adsorption of benzene, toluene, ethylbenzene and p-xylene by NaOCl-oxidized carbon nanotubes, Colloid, Surfaces A 353 (2010) 83–91.
[75] R. Andreozzi, V. Caprio, A. Insola, R. Marotta, R. Sanchirico, Advanced oxidation processes for the treatment of mineral oil-contaminated wastewaters, Water Res. 34 (2000) 620–628.
[76] T. Garoma, M.D. Gurol, O. Osibodu, L. Thotakura, Treatment of groundwater contaminated with gasoline components by an ozone/UV process, Chemosphere 73 (2008) 825–831.
[77] E. Metcalf, F.L. Burton, H.D. Stensel, G. Tchobanoglous, Wastewater engineering: treatment and reuse, McGraw Hill, 2003.
[78] H. Dehouli, O. Chedeville, B. Cagnon, V. Caqueret, C. Porte, Influences of pH, temperature and activated carbon properties on the interaction ozone/activated carbon for a wastewater treatment process, Desalination 254 (2010) 12–16.
[79] H. Valdes, F. Murillo, J. Manoli, C. Zaror, Heterogeneous catalytic ozonation of benzothiazole aqueous solution promoted by volcanic sand, J. Hazard. Mater. 153 (2008) 1036–1042.
[80] H. Valdés, V.J. Farfán, J.A. Manoli, C.A. Zaror, Catalytic ozone aqueous decomposition promoted by natural zeolite and volcanic sand, J. Hazard. Mater. 165 (2009) 915–922.
[81] S. Mortazavi, G. Asgari, S. Hashemian, G. Moussavi, Degradation of humic acids through heterogeneous catalytic ozonation with bone charcoal, React. Kinet. Mech. Cat. 100 (2010) 471–485.
[82] T. Zhang, J. Ma, J. Lu, Z. Chen, C. Li, J. Jiang, Catalytic ozonation with metal oxides: an option to control THM formation potential, Water Sci. Tech-W Sup. 6 (2006) 63–70.
[83] B. Kasprzyk-Hordern, Chemistry of alumina, reactions in aqueous solution and its application in water treatment, Adv, Colloid. Interface 110 (2004) 19–48.
[84] F. Qi, B. Xu, Z. Chen, J. Ma, D. Sun, L. Zhang, Influence of aluminum oxides surface properties on catalyzed ozonation of 2, 4, 6-trichloroanisole, Sep. Purif. Technol. 66 (2009) 405–410.
[85] C. F. Forster, Wastewater Treatment and Technology, Thomas Telford, London (2003).
[86] M.J. O'Neil, The Merck index: An encyclopedia of chemicals, drugs, and biologicals, 15th Ed. Royal Society of Chemistry (2013).
[87] R.N. Yong, S. Rao, Mechanistic evaluation of mitigation of petroleum hydrocarbon contamination by soil medium, Can. Geotech. J. 28 (1991) 84–91.
[88] L. Mohammadi, A. Rahdar, E. Bazrafshan, H. Dahmardeh, M.A.B. Hasan Susan, G.Z. Kyzas, Petroleum hydrocarbon removal from wastewaters: A review, Processes 8 (2020) 447.